

RESEARCH ARTICLE

Expression of the inactivating deiodinase, Deiodinase 3, in the pre-metamorphic tadpole retina

Karine Le Blay^{1*}, Laëtitia Préau², Ghislaine Morvan-Dubois^{1☯‡*}, Barbara Demeneix^{1☯‡*}

1 Département Adaptation du Vivant, UMR CNRS, Evolution des Régulations Endocriniennes, Muséum National d'Histoire Naturelle, Paris, France, **2** Zoologisches Institut, Zell-und Entwicklungsbiologie, Karlsruhe Institute of Technology (KIT), Karlsruhe, Germany

☯ These authors contributed equally to this work.

☯ Current address: Neuroscience Paris Seine—IBPS, Sorbonne Universities, CNRS UMR8246, Inserm U1130, UPMC, Paris, France.

‡ These authors are co-senior authors on this work.

* le.blay@mnhn.fr (KL); bdem@mnhn.fr (BD); ghislaine.morvan-dubois@upmc.fr (GM-D)



OPEN ACCESS

Citation: Le Blay K, Préau L, Morvan-Dubois G, Demeneix B (2018) Expression of the inactivating deiodinase, Deiodinase 3, in the pre-metamorphic tadpole retina. PLoS ONE 13(4): e0195374. <https://doi.org/10.1371/journal.pone.0195374>

Editor: Anand Swaroop, National Eye Institute, UNITED STATES

Received: July 7, 2017

Accepted: March 21, 2018

Published: April 11, 2018

Copyright: © 2018 Le Blay et al. This is an open access article distributed under the terms of the [Creative Commons Attribution License](https://creativecommons.org/licenses/by/4.0/), which permits unrestricted use, distribution, and reproduction in any medium, provided the original author and source are credited.

Data Availability Statement: All relevant data are within the paper.

Funding: This work was supported by the Centre National de la Recherche Scientifique (CNRS), the Museum National d'Histoire Naturelle (MNHN), the French ANR "Thrust," Agence Nationale de la Recherche (11BSV2019 02) and a PERSU grant (SU-14-R-PERSU-04) to BAD. Laëtitia Préau received a PhD grant from the French Ministry of Research and Education and support from the PERSU grant (Ministère de l'Éducation Nationale, de l'Enseignement Supérieur et de la Recherche)

Abstract

Thyroid hormone (TH) orchestrates amphibian metamorphosis. Thus, this developmental phase is often used to study TH-dependent responses in specific tissues. However, TH signaling appears early in development raising the question of the control of TH availability in specific cell types prior to metamorphosis. TH availability is under strict temporal and tissue-specific control by deiodinases. We examined the expression of the TH-inactivating enzyme, deiodinase type 3 (D3), during early retinal development. To this end we created a *Xenopus laevis* transgenic line expressing GFP from the *Xenopus dio3* promoter region (*pdio3*) and followed *pdio3*–GFP expression in pre-metamorphic tadpoles. To validate retinal GFP expression in the transgenic line as a function of *dio3* promoter activity, we used *in situ* hybridization to compare endogenous *dio3* expression to reporter-driven GFP activity. Retinal expression of *dio3* increased during pre-metamorphosis through stages NF41, 45 and 48. Both sets of results show *dio3* to have cell-specific, dynamic expression in the pre-metamorphic retina. At stage NF48, *dio3* expression co-localised with markers for photoreceptors, rods, Opsin-S cones and bipolar neurons. In contrast, in post-metamorphic juveniles *dio3* expression was reduced and spatially confined to certain photoreceptors and amacrine cells. We compared *dio3* expression at stages NF41 and NF48 with TH-dependent transcriptional responses using another transgenic reporter line: *THbZIP*-GFP and by analyzing the expression of T₃-regulated genes in distinct TH availability contexts. At stage NF48, the majority of retinal cells expressing *dio3* were negative for T₃ signaling. Notably, most ganglion cells were virtually both *dio3*-free and T₃-responsive. The results show that *dio3* can reduce TH availability at the cellular scale. Further, a reduction in *dio3* expression can trigger fine-tuned T₃ action in cell-type specific maturation at the right time, as exemplified here in photoreceptor survival in the pre-metamorphic retina.

(SU-14-R-PERSU-04) to BAD. The funders had no role in study design, data collection and analysis, decision to publish, or preparation of the manuscript.

Competing interests: The authors have declared that no competing interests exist.

Abbreviations: TH, Thyroid hormone; D3, deiodinase type 3; T4, thyroxine; T3, triiodothyronine; TR, TH receptors; D2, deiodinase type 2; PBS, phosphate buffer saline; NGS, normal goat serum; ISH, in situ hybridization; SSC, saline sodium chloride citrate; GFP, green fluorescent protein; INL, inner nuclear cells layer; ONL, outer nuclear cells layer; OPL, outer plexiform layer; IPL, inner plexiform layer; NF, Nieuwkoop and Faber; TH/bZIP, Thyroid Hormone basic leucine zipper; Chx10, Ceh-10 Homeodomain-Containing Homolog; CMZ, ciliary marginal zone; Opsin S, Opsin Short wavelength; Opsin M, Opsin Medium wavelength; UVS cones, ultraviolet sensitive cones.

Introduction

Tissue specific availability of the two main forms of thyroid hormone, thyroxine (T₄) and the most biologically active form, triiodothyronine (T₃), orchestrates the complex developmental program of amphibian metamorphosis. As in other vertebrates, development of the central nervous system is highly T₃-dependent [1]. This is the case for retinal development, [2, 3]. TH receptors (TR), TRa and TRb, have been detected in the retina of mice, chicken and the African clawed frog *Xenopus laevis* [4, 5]. We previously showed that disrupting *thrb* receptor during development impairs *Xenopus* retinal formation [4]. More specifically, inducing a mutation in *Xenopus laevis thrb* ligand binding domain causes defects in eye development in embryos [4]. These data suggested that TH could have tissue specific responses during early stages of eye development. However, nothing is known on the cell specific role of TH in amphibian eye development at pre-metamorphic stages and whether certain cell types would be particularly sensitive to excess T₃.

Thyroid hormone availability in specific tissues is determined by reciprocal activity of activating and inactivating deiodinases. The main activating deiodinase is deiodinase 2 (D2), whereas deiodinase 3 (D3, encoded by *dio3*) is the principal inactivating enzyme in tissue. Deiodinases are essential regulators of TH levels in target cells, notably in the nervous system [6, 7, 8]. The central role of deiodinases in controlling TH availability is exemplified by control of retinal development in multiple vertebrate species [5, 9, 10, 11]. In particular, fine regulation of TH availability by activating and inactivating deiodinases ensures survival and maturation of cone photoreceptors in mice [12]. Deiodinase knockdown in zebrafish eye affects eye size, retinal lamination and strongly reduces the number of rods and cone cells [5]. This result is consistent with the lamination defect observed when impairing deiodinase activity with iopanoic acid in earlier pre-metamorphic *Xenopus* embryos [4]. When TH deiodination is impaired by iopanoic acid treatment, T₃ treatment further enhances the deleterious eye phenotype, revealing a crucial role for *thra* as aporeceptor and pinpointing that TH availability is tightly controlled [4] during eye development. D3 plays an essential protective role in inhibiting TH-induced proliferation in CMZ, resulting in an asymmetric growth in *Xenopus laevis* retina during metamorphosis [13, 11], or in protecting certain photoreceptors from excessive T₃ signaling in the mouse and zebrafish retina [5, 12, 14]. These findings favor the hypothesis of a control of local TH availability mostly by the inactivating deiodinase D3.

The second question raised by this data set is the scale at which local TH availability is controlled, and more precisely, if the control occurs at the tissue level or cellular level. TH roles in proliferation and in the differentiation of cone photoreceptors are well known, but little is known about the protective role of D3 during retinal neurogenesis.

Furthermore, previous studies in *Xenopus* retina addressed the question of the regulation of the stem cells and progenitor cells proliferation [15] or the genesis of different cell types [16, 17, 18, 19] in early development. Other studies addressed the determination of cone and rod photoreceptors during embryonic stages NF33-41 [20, 21]. These studies raised the importance of local environment and extrinsic factors but did not address the role of TH.

As to other species, the role of TH on retinal development has been addressed during embryogenesis in rodents [10, 14], during pro-metamorphosis in fish [5] as well as during metamorphosis in *Xenopus* [4, 11].

As to deiodinase expression, different studies have shown the general pattern expression of *dio3* during embryonic chicken brain development [3, 12] and increasing mRNA levels during zebrafish embryonic development [5, 9] and in brain between stages NF45 and NF48 in *Xenopus* tadpoles [8]. But, no studies have addressed the control of TH availability by D3 on retinal neurogenesis in *Xenopus* pre-metamorphic tadpoles.

To address the question of TH availability in specific retinal cell types, we used a number of complementary experimental approaches. First, we compared expression of *dio3* using both *in situ* hybridization (ISH) and exploiting a *pdio3*-GFP construct, where GFP expression is controlled by part of the *Xenopus dio3* promoter. Second, we compared *dio3* ISH expression with immunohistochemistry for specific retinal cell types. Third, we determined which of these cell types responded to T₃ signaling by using a well-established *TH/bZIP*-GFP reporter system [22, 23, 24]. Taken together, the results show that *dio3* expression could limit T₃-dependent responses in specific retinal cells at specific developmental stages.

Material and methods

1. Transgenic and wild type animals

X. laevis tadpoles and juveniles were obtained by in-house breeding. To obtain eggs, adult frogs were injected with human chorionic gonadotropin (Chorulon) (400 U/female and 200 U/male). Some adult frogs were bought to the CRB (Xenope Biology Resources Centre, Centre de Resource Biologie Xenope), France (University of Rennes1; <http://xenopus.univ-rennes1.fr/>). Animals were reared under a 12-hour light/12-hour dark cycle at 22–23°C. Animals were staged according to Nieuwkoop and Faber (NF) (1956). Juveniles were used when they had developed beyond NF66 and weighed between 1 and 2 g.

To determine T₃ responsiveness in the retina, we used the *X. laevis* transgenic *TH/bZIP* reporter line [22, 23, 24]. The transgenic *TH/bZIP* reporter line contains a series of T₃ sensitive response elements upstream of the GFP coding sequence providing a direct T₃ readout. F1 founders were crossed together to produce F2 homozygous transgenic tadpoles.

All animal studies were carried out in accordance with the European Union regulations concerning the protection of experimental animals and approved by the Museum National d'histoire Naturelle Animal Care and Use Committee, Paris, France. All procedures were approved by the institutional Ethics Committee (Animal Housing Agreement Number: C75-05-01-2, Committee Approval 68.031).

2. Generation of the *Xenopus laevis* deiodinase 3–GFP transgenic line

The *X. laevis* transgenic line *deiodinase 3*-GFP (*pdio3*-GFP) reporter was obtained by sperm nuclei-mediated REMI method transgenesis [25] using a *dio3* promoter driven-GFP expressing construct. Injections were carried out so that the transgene was inserted into the genome prior to the first cleavage. The DNA plasmid construct used for this reporter line corresponds to a clone representing a part of the *Xenopus tropicalis* *dio3* promoter locus and upstream regulatory elements. The DNA clone represents 1448 pb of the full *Xt dio3* 4915 pb promoter locus. The cDNA clone was from 454 pb of the 3' end *Xt dio3* promoter locus. The PCR product was initially obtained with the ExTaq TaKaRa kit (Ozyme, ref: TAKRR013A) from *X. tropicalis* tadpole tail genomic DNA extract. PCR primers were designed against the promoter *dio3* locus. Forward and reverse primers were 5' CGGGGAAGATATGTGAAGGA3' and 5' GGGCTCCCAGGATGATCTGA 3', respectively. The latest *Xenopus tropicalis* genome annotation, confirms the position of the clone in the promoter. This PCR product was sub-cloned into a pGlow-GFP vector (Invitrogen pGlowTOPO cloning kit ref: 45–0021) and verified by sequencing. F0 or F1 transgenic founders were crossed with wild type adult to produce F1 or F2 transgenic tadpoles that were used for the characterization experiments.

3. Tadpole treatment

The *X. laevis* transgenic (*pdio3*-GFP) reporter tadpoles NF48 were treated for 24 h, with 10^{-8} M T_3 (Sigma, St Quentin Fallavier, France), with 5.10^{-6} M IOP (TCI Europe, Zwijndrecht, Belgium) or with 10^{-8} M T_3 + 5.10^{-6} M IOP (diluted in 0.1% ethanol) [4]. Vehicle control group is used in 0.1% ethanol. The experiment was performed twice, with 5–8 animals per group.

4. Sample collection and preparation

Tadpoles and juveniles of both transgenic reporter lines were deeply anesthetized by submersion in 0.1% tricaine methanesulfonate anesthesia (MS-222, Sigma-Aldrich) and euthanized by decapitation. Whole heads of NF48 tadpoles and juveniles were fixed overnight at 4°C in 4% paraformaldehyde (PFA, Sigma-Aldrich, Saint Quentin Fallavier, France) in phosphate buffered saline (PBS pH 7.4). Samples were briefly washed three times (15 min.) in PBS and placed overnight in 15% sucrose PBS. Samples were embedded in Tissue-Tek and stored at -80°C. Coronal cryosections (16 micrometers) were performed on whole heads and analyzed on eyes. Sections were stored at -80°C prior to immunohistochemistry or *in situ* hybridization.

5. Immunohistochemistry for GFP and Opsin Blue, GFP and Rhodopsin, GFP and ChX10

Coronal whole heads cryosections were briefly rehydrated with phosphate buffer salt PBS (pH 7.4) and Tween 20 (0.1%), then post-fixed with 4% PFA for 10 min. Sections were washed in PBS-Tween 20 (0.1%) and blocked with 10% normal goat serum in PBS-Tween 20 (0.1%) (both from Sigma-Aldrich) to reduce non-specific binding. Sections were then incubated overnight at 4°C with primary antibody chicken polyclonal GFP (Abcam, Ab 13970) or rabbit polyclonal GFP (Invitrogen, ref: 11122) diluted 1:300 in PBS-Tween 20 (0.1%) containing 5% normal goat serum (NGS), according to the species in which the second primary antibody was generated. The slides were rinsed with fresh PBS-Tween 20 (0.1%) and incubated two hours at room temperature (RT) with secondary antibody (Alexa fluor 488 goat anti-rabbit, Invitrogen A-11034 Carlsbad, CA, USA) diluted 1:500 in PBS-5% normal goat serum-0.1% Tween 20. Then, sections were incubated with the second primary rabbit polyclonal antibody either Opsin Blue, a marker of Opsin S (Millipore AB 5407) diluted 1:250 or mouse monoclonal Rhodopsin (Sigma-Aldrich R 5403) diluted 1:500 or sheep polyclonal ChX10 (Exalpha X1180P) diluted 1:200 in PBS-Tween 20 (0.1%) containing 5% normal goat serum. Slides were rinsed with fresh PBS-Tween 20 (0.1%) and incubated two hours at RT with secondary antibody Alexa fluor 568 goat anti-rabbit, (Invitrogen A-11036) for Opsin-Blue or Alexa fluor 594 donkey anti-mouse, (Invitrogen A-21203) for Rhodopsin or Alexa 594 donkey anti-sheep IgG (Invitrogen A-11016) for ChX10 diluted 1:500 in PBS-Tween 20 (0.1%) with 5% NGS. Immunostained retinas were rinsed several times in PBS-Tween 20 (0.1%) and mounted with Prolong Gold antifade reagent with DAPI (Invitrogen P-36931) and a cover slip.

6. Immunohistochemistry for GFP and GABA or GFP and Parvalbumin

Coronal cryosections were briefly rehydrated with phosphate buffer salt PBS (pH 7.4) and Triton X-100 (0.3%). Sections were blocked with 10% normal goat serum in PBS-Triton X-100 (0.3%) (both from Sigma-Aldrich) to reduce non-specific binding during 2 hours at room temperature. Sections were then incubated overnight at 4°C with primary antibody chicken polyclonal GFP (Abcam, Ab 13970) diluted 1:300 in PBS-Triton X-100 (0.3%) containing 5% normal goat serum (NGS). The slides were rinsed with fresh PBS-Tween 20 (0.1%) and incubated two hours at room temperature (RT) with secondary antibody (Alexa fluor 488 goat

anti-chicken, Invitrogen A-11039 Carlsbad, CA, USA) diluted 1:500 in PBS-5% normal goat serum-0.3% Triton X-100. Then, sections were incubated with the second primary rabbit polyclonal antibody GABA, gamma-Aminobutyric Acid (Immunostar 20094) diluted 1:1500 or mouse monoclonal Parvalbumin IgG1 (Millipore MAB1572) diluted 1:100 in PBS-Triton X-100 (0.3%) containing 5% normal goat serum. Slides were rinsed with fresh PBS-Tween 20 (0.1%) and incubated two hours at RT with secondary antibody Alexa fluor 647 goat anti-rabbit, (Invitrogen A-21245) for GABA or Alexa fluor 568 goat anti-mouse IgG1, (Invitrogen A-21124) for Parvalbumin diluted 1:500 in PBS-Triton X-100 (0.3%) with 5% NGS. Immunostained retinas were rinsed several times in PBS-Tween 20 (0.1%) and stained by DAPI (Sigma-Aldrich) for 7 min, rinsed several times in PBS-Tween 20 (0.1%), another time and mounted with Prolong Gold antifade reagent (Invitrogen P-36930) and a cover slip.

The immunostained retinas were visualized with a LEICA DM 5500 B microscope equipped with a LEICA CTR 5500 lens and for epifluorescence with a PRIOR Lumen 200 system. Fluorescent image acquisitions were carried out using a ZEISS LSM 710 system confocal microscope by channels or spectral mode acquisitions and the Zen 2011 software acquisition at the J. Monod Institute (ImagoSeine platform, Jussieu University, Paris, France).

7. *In situ* Hybridization (ISH)

Probes for *dio3* cDNA were isolated by RT-PCR using a pool of RNA extracted from embryos and tadpoles at several stages. The PCR fragment for *pdio3* (296 bp, forward: TCGGTGCACAA TAGTCGGG and reverse:CTTCTGCCCCGTGCCACAC) were cloned using the TOPO TA cloning kit dual promoter (Invitrogen, Carlsbad, CA, USA) and sequenced to check orientation. The *dio3* mRNA probe was synthesized using T7 enzyme 25 (Roche, Basel, Switzerland) and labeled with digoxigenin (Roche, Basel, Switzerland). ISH was performed on cryosections. Slides were briefly rehydrated with PBS (pH 7.4) then post-fixed with 4% PFA during 10 min. Then slides were washed with PBS Tween 20 (0.1%). Tissues were permeated with proteinase k (5.10^{-6} g/ml, Sigma, ref. P4850) for two minutes. Slides were then post-fixed with 4% PFA during 10 min followed by wash with PBS Tween 20 (0.1%). To prevent RNA interaction with protein, slides were incubated with 100 mM Triethanolamine/0.25% anhydride acid acetic during 10 min. Slides were washed with PBS Tween 20 (0.1%) and then pre-hydrated with hybridization buffer (formamide 50%, SSC 5X, ARNt grade VI à 1 mg/ml, heparin 100.10^{-6} g/ml, Denhart's 1X, Tween 20 (0.1%), CHAPS 10 mM 0.1%, EDTA 10 mM) during 1 hour. After denaturation *dio3* probe was used at 1 ng/ μ l concentration and incubated on slides overnight at 60°C. Slides were washed several times with SSC buffer (saline sodium chloride citrate Sigma, ref.93017) at 65°C and then blocked with 10% NGS conjugated to alkaline phosphatase (1/2000, Roche) in 5% NGS/PBS/Tween 20 (0.1%). Slides were washed several times in maleic acid buffer. Signals were revealed using BM purple (Roche, ref.11442074001). Reactions were stopped by washes with PBS Tween 20 (0.1%). Slides were mounted with Prolong (Invitrogen, Carlsbad, CA, USA). ISH on retina sections was visualized using a LEICA DM 5500 B microscope equipped for visible light with LEICA CTR 5500. Image acquisition exploited a DFC 450 C Camera and the Leica Application suite LAS version 4.1.0 software acquisition.

8. RNA isolation and reverse transcription (RT)

RNA extraction was performed by RNA isolation from micro-scale, using RNAqueous Micro kit (Invitrogen AM 1931). For mRNA extraction from eyes, two steel balls were used for each sample in 100 microliters of lysis solution. Eyes were homogenized by using a tissue lyser at 30 Hz twice during 1 min. Ethanol 100% (50 microliters) was added and the lysate was placed on a micro-filter cartridge before centrifugation (16,400 x g, 20 sec.). The cartridge was rinsed

three times with a wash solution before RNA elution. A warm (75°C) RNA elution solution (18 microliters) was used before centrifugation (twice 16,400 x g, 30 sec. at room temperature). A DNase was used (22 min. at 37°C) and an inactivation reagent was added before centrifugation (16,400 x g, 2 min.). Concentrations of RNA were determined by using a NanoDrop (ThermoScientific, Rockford, IL). RNAs were stored in TRIS 10 mM /EDTA 0.1 mM (PH 7.4) at -80°C.

Extracted total RNA (300 ng) was used for reverse transcription (RT) using a High Capacity cDNA RT kit (Applied Biosystems, Foster City, CA) with the addition of RNase inhibitor. A control for genomic DNA (RT- reaction: all reagents and RNA except reverse transcriptase) was performed for each group (Ctrl, T₃, IOP, IOP+T₃).

9. Real-time PCR quantification

The amount of each RNA transcript was estimated by relative quantitative real-time PCR (qRT-PCR) using Power SYBR green master mix and a Quant Studio Flex 6 (Applied Biosystems). 5 to 8 biological replicates were performed for each group. A 1:10 dilution of each cDNA was run in triplicate on a 384-well plate for each primer pair (Table 1) (intra assay variability) by using thermal cycling parameters: 95°C for 10 min, 95°C for 15 sec and 60°C for 1 min (40 cycles) and an additional step for dissociation curves was performed for all plates. Results were normalized with the expression of reference gene *odc*. DDCT method was used to estimate fold change of expression when compared to the untreated (CTL) group. PCR primer sequences are designed previously [26] for the housekeeping gene *odc*. Primers list is provided in Table 1.

Statistical analysis

For multiple comparison analysis, Non-parametric ANOVA was performed, followed by a Kruskal Wallis test (PRISM7). Heatmap was performed on Fold Changes (PRISM7), and correlation analysis was performed on XLSTAT.

Results

Dynamic expression of retinal *dio3* in the pre-metamorphic *Xenopus laevis* retina

To address the role of *dio3* in pre-metamorphic retina, we cloned part of the *X. tropicalis dio3* promoter and generated a transgenic *pdio3*-GFP reporter line. GFP immunostaining was used to follow *pdio3*-reporter GFP expression. To validate the *dio3* transgenic GFP reporter signal in the retina, we compared it to the endogenous signal obtained with ISH using antisense

Table 1. Primers list.

Gene	Primer sequences	
	Forward primer	Reverse primer
<i>eGFP</i>	5' ACA GGA TGA GGA TCG TTT CG 3'	5' TGT CTG TTG TGC CCA GTC AT 3'
<i>dio3</i>	5' CAC AAA AAG TGC GAC CAA ACG 3'	5' GCC TTG TTG CAG TTT ACT 3'
<i>thrb</i>	5' ATA GTT AAT GCG CCC GAG GGT GGA 3'	5' CTT TTC TAT TCT CTC TCC ACG CTA GC 3'
<i>thibz</i>	5' CCC GTC TCC GTG CTG AAC T 3'	5' GGT CAC GTA CCA GGC CAA A 3'
<i>klf9</i>	5' TGT GGC AAA GTT TAT GGG AAG TCT 3'	5' GGC GTT CAC CTG TAT GGA CTC T 3'
<i>odc</i>	5' GCT TCT GGA GCG GGC AAA GGA 3'	5' CCA AGC TCA GCC CCC ATG TCA 3'

<https://doi.org/10.1371/journal.pone.0195374.t001>

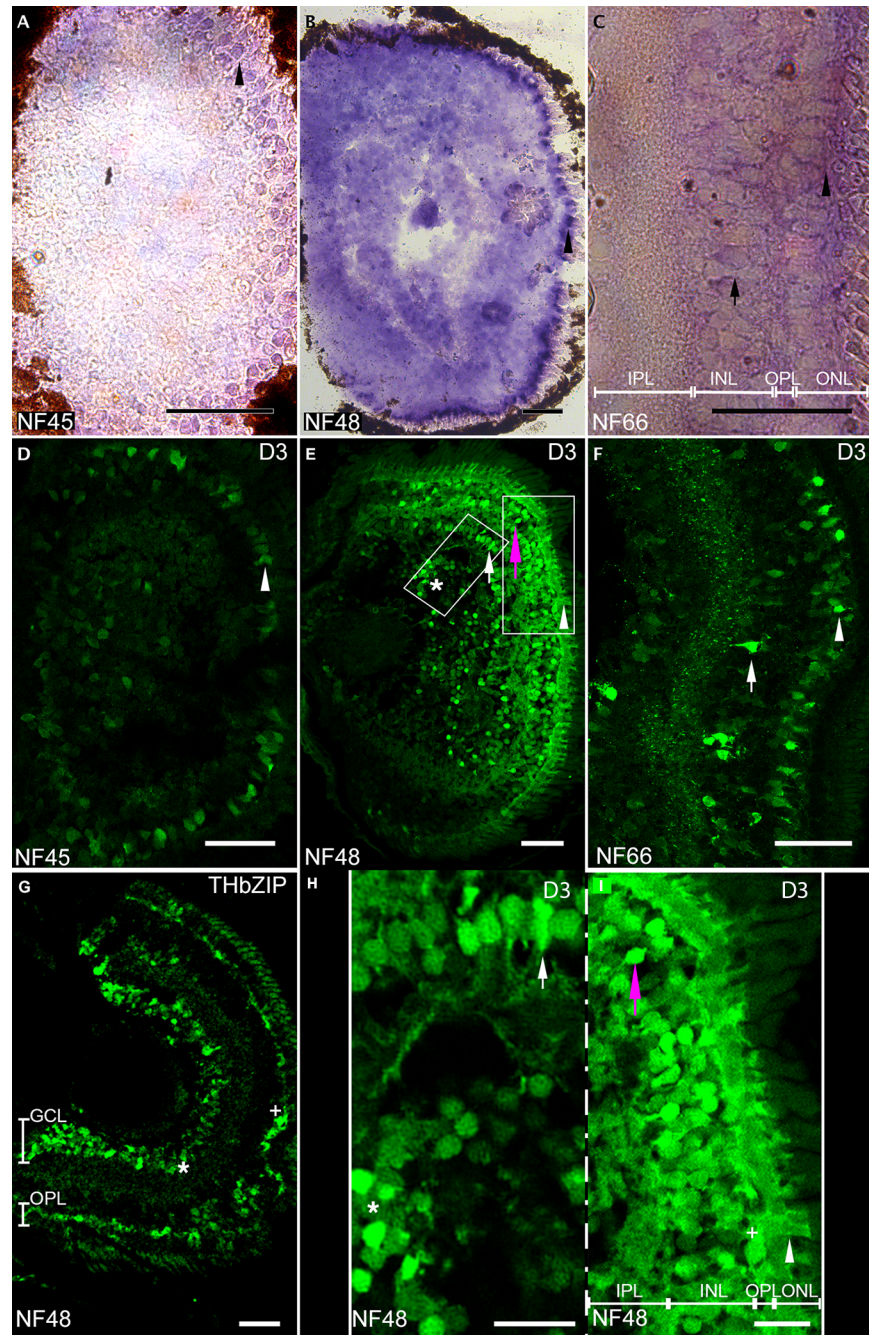


Fig 1. Comparison of GFP expression in transgenic *pdio3* reporter line to endogenous *dio3* expression. Fig 1A–1C: Endogenous *dio3* in situ hybridization on retina coronal sections from animals at NF45 (Fig 1A), NF48 (Fig 1B), NF66 (Fig 1C) stages. Fig 1D–1F: GFP immuno-labeling on retina coronal sections at NF45 (Fig 1D), NF48 (Fig 1E, 1H and 1I), NF66 (Fig 1F) stages. Comparison of GFP expression between tadpoles from the *pdio3* transgenic line (Fig 1E) and from *TH/bZIP* transgenic T_3 reporter tadpoles at NF48 stage (Fig 1G). Orientation is with lens on the left and retina on the right. Photoreceptor cell bodies (arrow head: Fig 1A–1F and 1I). Amacrine cells (arrow: Fig 1C, 1F, 1E and 1H). Bipolar neurons (magenta arrow: Fig 1E and 1I). Ganglion cells (asterisk: Fig 1E, 1H and 1G). Scale bars: 50 microns.

<https://doi.org/10.1371/journal.pone.0195374.g001>

probes against *dio3* (Fig 1A–1F). Expression of *dio3* (Fig 1A and 1B) and *pdio3*-reporter GFP

(Fig 1D, 1E, 1H and 1I) were examined by ISH on head cryo-sections in tadpoles at stages NF45 and NF48 and in the froglet at stage NF66 (Fig 1C and 1F).

At stage NF45, both the *dio3* ISH signal and GFP expression were limited to a very few ganglion cells and in a subset of the photoreceptors of the outer nuclear layer, as judged by cell morphology and anatomical localization (Fig 1A and 1D). At stage NF48, both the *dio3* ISH signal and GFP expression showed higher intensity and a wider distribution, being present in all retinal cell types: ganglion cells, inner nuclear layer cells (bipolar neurons, horizontal neurons and amacrine cells) and in the outer nuclear layer cells (basal part of the photoreceptors) (Fig 1B, 1E, 1H and 1I). Cell morphologies were determined according to Wong et al. [27]. At stage NF66 corresponding to a post-metamorphic juvenile stage, *dio3* expression was more restricted and localized in the outer nuclear layer and in the inner nuclear layer. More specifically, both ISH and GFP immunocytochemistry showed *dio3* expression in certain photoreceptor types and in Amacrine cells (Fig 1C and 1F).

D3 expression generally corresponds to lack of T₃ responsiveness

To determine which retinal cells express D3 and those that respond to T₃, we compared the GFP expression in F2 tadpoles for two transgenic reporter lines, respectively *pdio3*-GFP and *TH/bZIP*-GFP. Retinal GFP immuno-labeling was examined on 16 micrometers coronal whole head cryo-sections at stage NF 41–42 (Fig 2) and NF48 (Fig 1E, 1H, 1I and 1G) (see Materials and Methods).

At stage NF41–42 D3 activity, as judged by GFP expression in *pdio3*-GFP tadpoles, is observed in numerous photoreceptors of the outer nuclear layer (yellow arrow heads, Fig 2A, 2C, 2E and 2F and Table 2) and in some bipolar neurons (blue arrow heads, Fig 2A, 2C, 2E and 2F and Table 2), whereas no T₃-response is detected in photoreceptors nor in bipolar neurons of the inner nuclear layer (INL) (Fig 2G, 2I, 2J and 2L and Table 2). Furthermore, the photoreceptors that are GFP positive in *pdio3*-GFP tadpoles are in the dorso-central area (Fig 2A).

The horizontal neurons (magenta arrow heads) of the outer plexiform layer that are GABA positive cells (Fig 2B and 2H) are also GFP positive in *pdio3*-GFP (Fig 2C and 2F and Table 2) and in *TH/bZIP* reporter tadpoles (Fig 2I, Table 2). Similarly, numerous amacrine cells (white arrow heads) in the inner nuclear layer, that are GABA/PARV positive cells (Fig 2B, 2D, 2H and 2K) are GFP positive in *pdio3*-GFP (Fig 2C, 2E and 2F and Table 2) and in *TH/bZIP*-GFP lines (Fig 2I and 2L and Table 2). However, they are less numerous in the *TH/bZIP* reporters. A ganglion cells subset (white asterisk) is Parvalbumine PARV positive (Fig 2D) in the ganglion cell layer and some of them are also GFP positive, in *pdio3*-GFP tadpoles (Fig 2E and 2F and Table 2). In *TH/bZIP*-GFP tadpoles, GFP expression is seen in a large subset of ganglion cells (Fig 2K and 2L and Table 2).

At stage NF48, widespread GFP expression was observed in *pdio3* tadpoles (Fig 1, 1E, 1H and 1I), a fact that was reflected by limited T₃ responses (lower *TH/bZIP*-driven GFP expression) notably in retinal ganglion cells, noted as “*” in Fig 1 and horizontal neurons (outer plexiform layer), noted as “+” (Fig 1G, Table 2). The *pdio3*-GFP expression displayed a strong dorso-ventral gradient (Fig 1E), which contrasted with the higher levels of *TH/bZIP*-driven GFP in the ventral area, mostly for the outer plexiform layer (Fig 1G). Thus, higher D3 levels appear to restrict T₃-responsiveness in the dorsal retina at this stage.

Furthermore, at this stage, no *TH/bZIP*-driven GFP signal was seen in any cell type in the inner nuclear layer as in bipolar neurons or amacrine cells (Fig 1G, Table 2), which corresponded to the high expression of *pdio3*-driven GFP at the same stage ((Fig 1E, 1H and 1I); note the magenta arrow indicating a bipolar neuron in Fig 1E and 1I and the white arrow indicating an amacrine cell in Fig 1E and 1H).

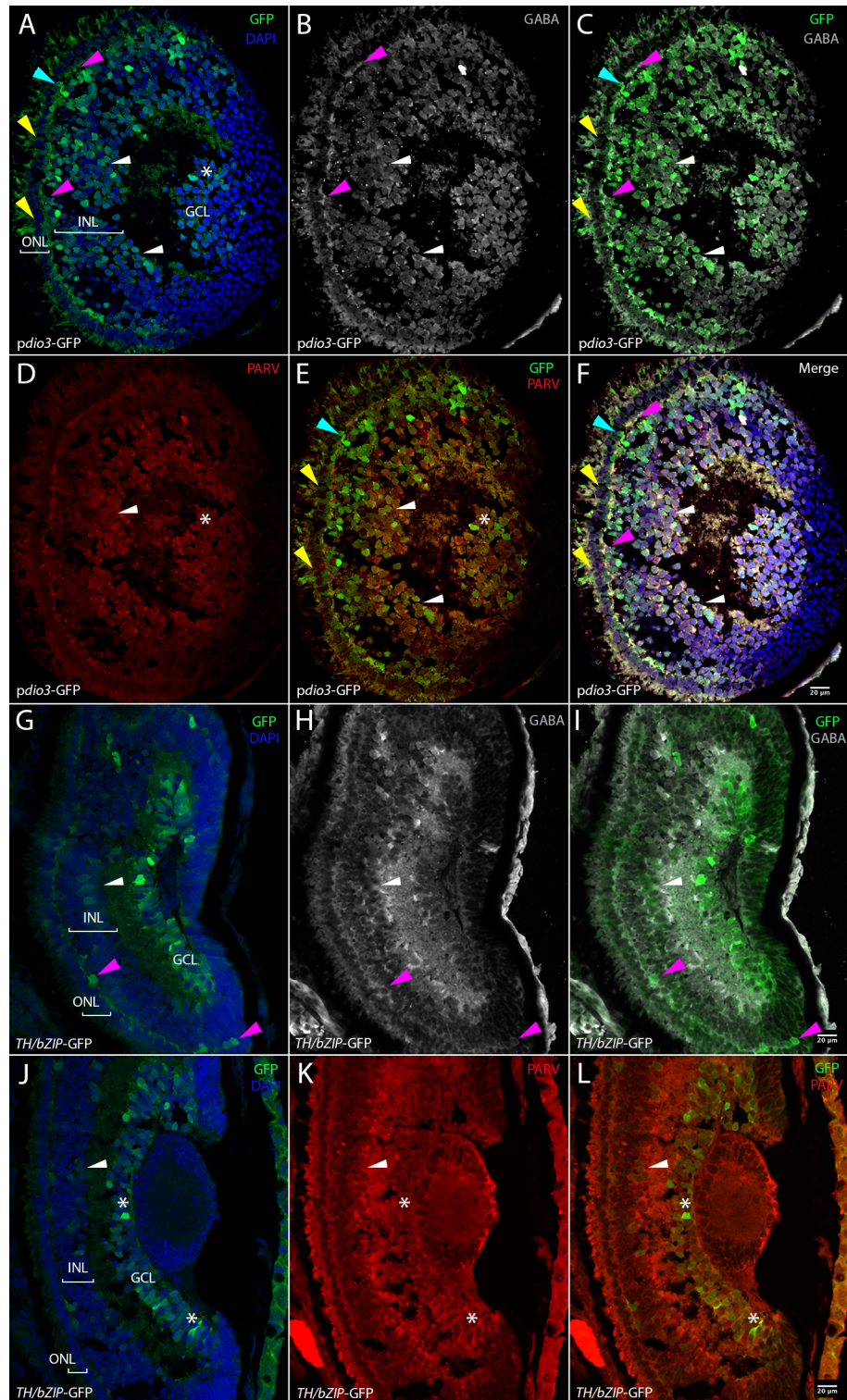


Fig 2. Comparison of *pdio3*-GFP and *TH/bZIP*-GFP expression pattern in NF41-42 reporter tadpoles. Fig 2A–2F: *pdio3*-GFP transgenic reporter tadpoles, Fig 2G–2L: *TH/bZIP*-GFP (T_3 sensor) reporter tadpoles. Fig 2A–2I: lateral plane sections. Fig 2J–2L: median plane section. Fig 2A, 2G and 2J: DAPI/GFP co-staining, Fig 2B and 2H: GABA labeling in horizontal neurons (magenta arrow heads) and amacrine cells (white arrow heads). Fig 2C and 2I: GFP/GABA co-labeling in horizontal neurons (magenta arrow heads) and amacrine cells (white arrow heads). Fig 2D and 2K: Parvalbumin PARV labeling in amacrine cells (white arrow head) and ganglion cells (asterisks). Fig 2E and 2L:

GFP/PARV co-labeling in amacrine cells (white arrow head) and ganglion cells (asterisks). Fig 2F: merge of all channels shown in Fig 2A–2E. Yellow arrow heads indicate photoreceptors and blue arrow heads indicate the bipolar neurons. Scale bars: 20 microns.

<https://doi.org/10.1371/journal.pone.0195374.g002>

Similarly, at stage NF48, the outer plexiform layer was GFP positive in both transgenic lines, reflecting a certain level of T₃ responsiveness despite discernable D3 activity. Indeed, some interneurons (horizontal cells, noted as “+”) respond to T₃ (Fig 1G, Table 2) and yet display limited *dio3* expression (Fig 1E and 1I and Table 2).

At stage NF48, most ganglion cells, (noted as “*”) did not express *dio3* and therefore could not respond to T₃ as confirmed by their positive *TH/bZIP* response (Fig 1G, Table 2). As expected, most photoreceptors express *dio3* (noted as “white head arrow in Fig 1E and 1I) and do not respond to T₃ (Fig 1G, Table 2). These results suggest that *dio3* expression limits T₃ responsiveness in specific cells too.

Opsin S-expressing cones, rods and bipolar neurons express *pdio33*-GFP at stage NF48

To determine more specifically in which retinal cell types *pdio3*-GFP expression was found we used double immunocytochemistry with established markers of each retinal cell type (see [Materials and Methods](#)). At stage NF48, *pdio3*-driven GFP expression was found to co-localize with markers of a large proportion of cone cells expressing Opsin Blue (Opsin S), noted by a magenta arrow in (Fig 3A, 3B and 3C), certain bipolar neurons (ChX10), noted by white head arrows (Fig 3D and 3H) and with all Rhodopsin positive rods, noted by white arrows (Fig 3E–3G).

Thus, as shown in Fig 3A, at stage NF48 GFP expression (green) was found in all retinal cell types in all layers, except in the ganglion cells layer where GFP expression is localized in few ganglion cells. In the outer nuclear layer, it only co-localizes with the body of the Opsin S cones (Fig 3A, in red). Co-localization of *pdio3*-GFP with several Opsin S cone body was observed and shown with magenta arrow in Fig 3B and 3C (zoom) (in red, with magenta arrow).

Another section revealed co-localization of GFP with Rhodopsin (in red), a specific marker of red rods (Fig 3E–3G for different magnifications). These results suggest that at stage NF48, *dio3* expression limits T₃ availability, thereby controlling Opsin S cones number and rods survival.

dio3 expression prevents induction of T₃-responsive genes

In order to determine whether *dio3* expression contributes to local control of TH availability in the developing eye, we treated NF48 *pdio3*-reporter tadpoles with T₃, IOP or IOP+T₃ (see [Materials and Methods](#) for details) and analyzed T₃ target genes expression (Table 1). A highly significant increase (p<0.001) in *dio3* expression was seen between IOP and IOP+T₃, but not between CTL and T₃ treated groups (Fig 4A). This difference in T₃ responsiveness can be interpreted in

Table 2. A summary of *pdio3*-GFP expression and T₃—responsiveness.

		TH/bZIP-GFP		pdio3-GFP	
		NF41	NF48	NF41	NF48
Outer Nuclear Layer	Photoreceptors	-	-	+	++
Inner Nuclear Layer	Bipolar neurons	-	-	+	+++
	Amacrine cells	+/-	-	+	+++
Ganglion Cell Layer	Retinal ganglion cells	++	+++	+	+/-
Outer Plexiform Layer	Horizontal cells dorsal zone	+	++	++	+++
	Horizontal cells ventral zone	++	+++	+	+

<https://doi.org/10.1371/journal.pone.0195374.t002>

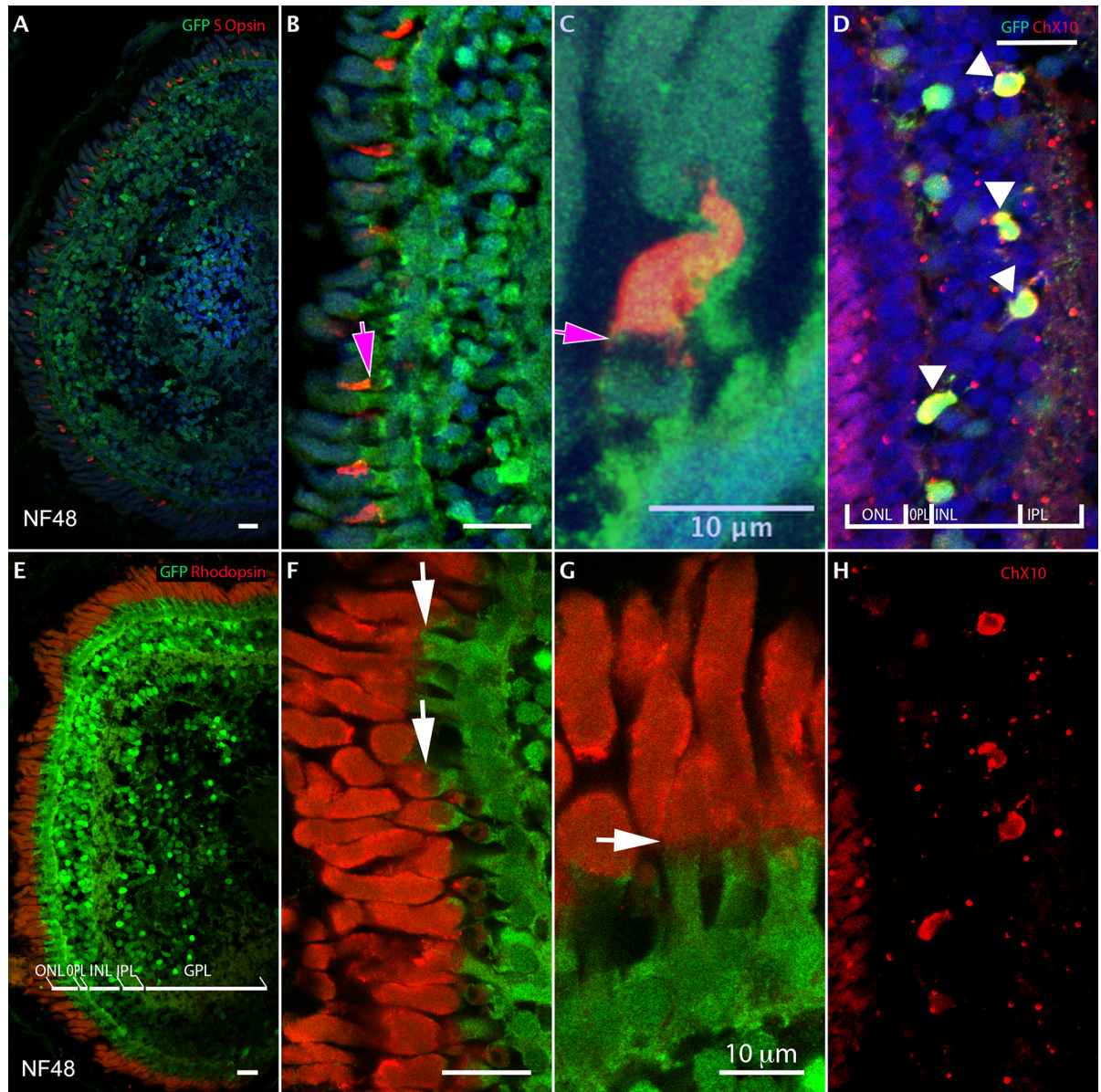


Fig 3. Multiple double-immuno-labeling with GFP (green) of *dio3* transgenic reporter line and Opsin-Blue or Rhodopsin or ChX10 (red) in NF 48 tadpoles. Opsin S cones co-expressing GFP and Opsin-S (Fig 3A–3C; magenta arrow: Opsin S cones; Fig 3B, 3C cone expressing GFP and apical cone expressing Opsin S). Rod cells co-expressing GFP and Rhodopsin (Fig 3E–3G; white arrow: rod Fig 3F and 3G body rod expressing GFP and apical rod expressing Rhodopsin). Bipolar neurons co-expressing GFP and ChX10 (white head arrow: Fig 3D, yellow cells); ChX10 channel from Fig 3D in Fig 3H. Scale bars: 20 microns (Fig 3A, 3B, 3D, 3E, 3F and 3H). Scale bars: 10 microns (Fig 3C and 3G).

<https://doi.org/10.1371/journal.pone.0195374.g003>

the light of the sensitivity of both activating and inactivating deiodinases to IOP [4] (Fig 4B). In the presence of T_3 , despite the presence of IOP, we observed an increased expression of the canonical T_3 -responsive genes *klf9* and *thibz*. Of note, IOP treatment itself, induces no significant change (as compared to controls) in *GFP*, *dio3* and T_3 target gene expression (Fig 4A). This result indicates that the local T_4 to T_3 conversion by D2 is insufficient to trigger T_3 target gene expression in the retina as a whole. In IOP+ T_3 treated group, *dio3*, *klf9*, *thibz* and *thrb* expression increases when compared to control group, showing that the cells expressing these genes are T_3 -

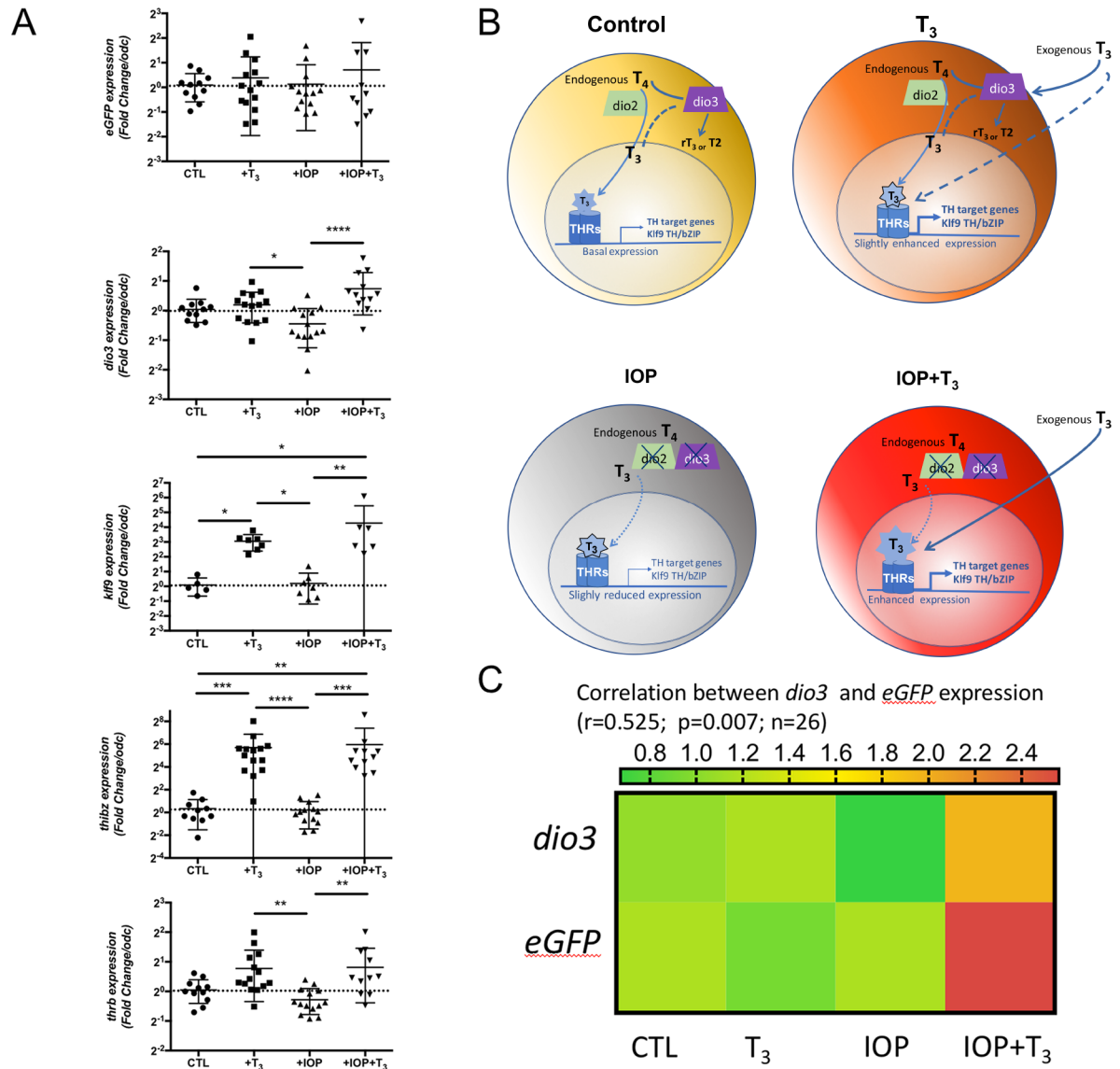


Fig 4. Expression of *dio3* contributes to modulate T₃ transcriptional response in the developing retina. Fig 4A. Real-time q-PCR analysis of *eGFP*, *dio3*, *klf9*, *thibz* and *thrb* for their T₃ transcriptional response in NF48 eye from reporter transgenic line *pdio3*-GFP. Gene expression was normalized against *odc*. mRNA levels from vehicle controls (CTL) were used as reference values. Results pooled from two to three independent experiments are represented as scatter dot plots mean with SD. 14 ≥ n ≥ 6 per group. Non-parametric ANOVA, Kruskal Wallis with uncorrected Dunn's test (PRISM7) was used to assess statistical significance. *, p < 0.05, **, p < 0.01; ***, p < 0.001. Fig 4B. Working model for the local control of T₃ local availability. Fig 4C. Heatmap of mean expression for each group illustrating the correlation between endogenous *dio3* expression and *eGFP* expression in *pdio3*-GFP tadpole retina.

<https://doi.org/10.1371/journal.pone.0195374.g004>

responsive. When comparing *dio3* and *GFP* expression (all observations pooled), a significant correlation (p = 0.007) is seen between *dio3* and *GFP* transcript levels (r = 0,525) (Fig 4C). This observation strengthens the argument that *GFP* can be used as an indicator of *dio3* expression levels.

Discussion

Several studies have shed light on the role of deiodinases in determining sensory organ development in vertebrates. This is especially the case in the eye, where TH-related development is

controlled by the timing of *Dio3* expression in mouse retina [12, 28] and *dio3* in *Zebrafish* eye [5], as well as in *Xenopus* retina during metamorphosis [11].

In mouse retina, *Dio3* is expressed in immature mouse retina. Ng et al. [12] showed that *Dio3*^{-/-} mice lost 80% of cones through neonatal cell death. Their results suggest that *Dio3* expression limits hormonal exposure of the cones ensuring cone survival and opsin (S and M) patterning, required for cone adaptive function during development. In zebrafish, knockdown of *dio3* by morpholinos causes reduced eye size and a strong reduction in rods and all four cones types. This result suggests the importance of *dio3* as a central player for zebrafish eye development. However, the roles of *dio3* on the survival and the patterning of Opsin type photoreceptors have not yet been addressed in *Xenopus* retina development, notably during pre-metamorphic stages. What is more, in *Xenopus*, there were no data on TH availability nor on the role of deiodinase 3 expression in other retinal cell types. Our experiments were designed to address these questions: how TH availability is controlled, and more precisely, if the control occurs at the tissue or cellular level and in which cells.

In the mouse retina, TH availability appears to control survival and patterning of specific retinal cells. Notably, a TH gradient is observed that may play a role in establishing the gradient of M-opsin [29]. In contrast, in *Xenopus* retina, there is a spatial gradient of *dio3* during metamorphosis, with a higher level in the dorsal retina [11]. These authors demonstrated that the dorsal ciliary margin zone (CMZ) cells are resistant to exogenous TH at stage 50–54, but they noted that an increase in proliferation of these cells was induced with a low concentration of T₃ when D3 activity was inhibited. In contrast, D3 overexpression inhibited TH-induced proliferation of the ventral CMZ cells [11]. This localized expression of *dio3* in the dorsal CMZ leads to the asymmetric growth of the frog retina, but the question of the role of *dio3* expression in the eyes of pre-metamorphic tadpoles was not addressed. Interestingly, in pre-metamorphic tadpoles, maximal *dio3* mRNA levels are found in whole tadpoles at NF46–NF48 stages [22], crucial stages before the first pro-metamorphosis stage NF 53, where generalized competence to respond to T₃ is observed [30].

Our study shows a specific and dynamic spatio-temporal pattern for *dio3* transcripts and *dio3* promoter activity in the retina of pre-metamorphic *Xenopus* tadpoles and post-metamorphic juveniles. The results suggest that the timing of retinal maturation in pre-metamorphic tadpoles is mostly controlled by local, cell-specific D3 activity following modulations between stages NF 41 and NF48. Moreover, D3 activity follows a dorso-ventral gradient at NF48. And the differential-T₃ responsiveness of retinal cells in our TH sensor model strongly suggests that some photoreceptors and bipolar neurons are more specifically protected from TH-driven maturation at stages NF41 and NF48. Likewise, the same result is observed for amacrine cells at NF48. Our results suggest too that more ventral horizontal neurons and more ganglion cells needed an active TH signaling between NF41 and NF48 (Fig 5).

Therefore, we show that in the pre-metamorphic retina, TH availability is not controlled at the tissue level but at the cellular level by D3, in most of the cell types in each retinal layer. In particular, D3 is expressed in photoreceptors and bipolar neurons at NF41 and NF48 whereas at NF45, only a photoreceptors subset expressed D3. At stage NF48, D3 is expressed specifically in Opsin S cones, rods and bipolar neurons (Fig 5).

The more restricted expression of D3 at stage NF45 could allow the recruitment and the maturation of more cell types of the inner nuclear layer and more pre-existing photoreceptors types. In parallel, maternal stocks of TH decrease at this stage [22]. Then, as the tadpole thyroid gland is formed, T₄ levels increase at NF46. So, we can speculate that the small subset of photoreceptors expressing D3 at NF45 may correspond to a subtype protected from TH maturation, just before TH levels increase.

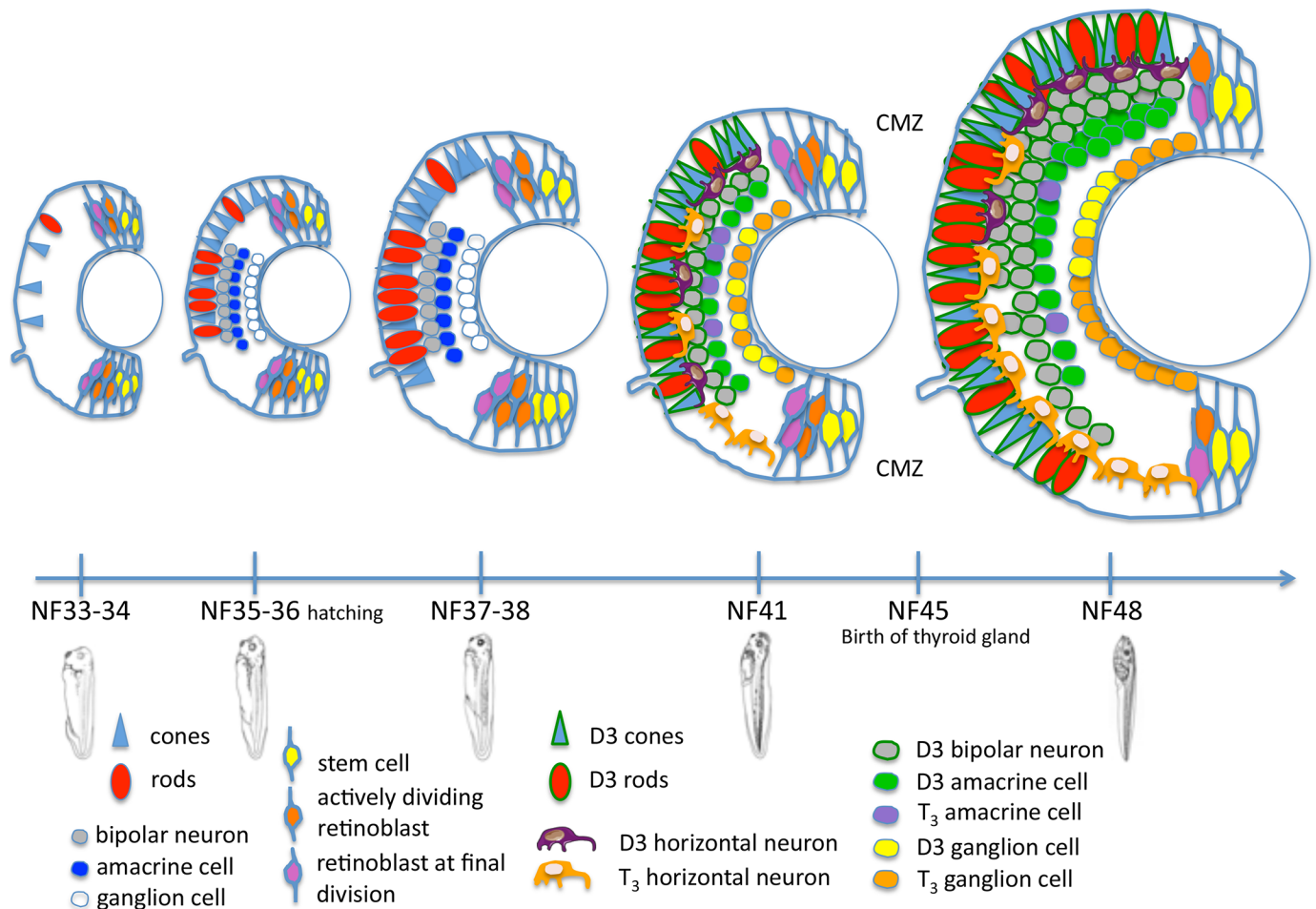


Fig 5. Retinal cell type neurogenesis in pre-metamorphic *Xenopus* from stage NF33 to stage NF48. The schema is based on the following references: Chang WS. and Harris WA. 1998, for photoreceptors determination from stages NF33 to NF41; Bilitou A. and Ohnuma S. 2010, for stem cells and retinoblasts from stages NF33 to NF41; Parker RO. et al. 2010, for violet cone opsin from stages NF35 to NF55; Dullin JP. et al. 2007, for horizontal and amacrine cells for stage NF40-41; Bessodes N. et al. 2017, for amacrine cells for NF41; Álvarez-Hernán G. et al. 2013, for ganglion cells for stage NF35-36; D’Autilia S. et al. 2006, for bipolar neurons for stage NF35-36 (in toto ISH). Results from the current study are used for the different retinal cell-types for stages NF41-48. The key to the different cell types legends is given within the schema.

<https://doi.org/10.1371/journal.pone.0195374.g005>

At stage NF48, the higher D3 expression observed in most photoreceptors and in cells of the inner nuclear cell layer, could be related to the fact that retina need to be protected from the step increase in TH levels that will initiate pro-metamorphosis at NF54 [31]. Pro-metamorphosis is a step where TH signaling is active and T₃-dependent tissue remodeling starts [30], illustrated by the onset of green rod differentiation in retina [21]. This result is in accordance with previous studies showing a retinal photoreceptors sensitivity to TH excess during retina development in several species. In vertebrates, TH and TRs are involved in opsin expression and cone development [10, 28, 32, 33, 34, 35]. Furthermore, TH can modulate the M-opsin/S-opsin ratio in the developing mouse retina [29]. Moreover, in trout, excess of TH during smoltification results in a loss of UVS cones [34, 36, 37, 38]. Likewise, another study shows that systemic TH may induce retinal remodelling in juvenile rainbow trout [39].

By analyzing *dio3* and T₃-target genes transcriptional regulation by T₃ in the presence or absence of a deiodinase inhibitor (IOP), we show that *dio3* plays a pivotal role in controlling local T₃ availability in *dio3* expressing cells. No effect of exogenous T₃ is observed when

deiodinases are not inactivated by IOP. The fact that expression of T_3 -responding genes increases when exogenous T_3 is added in the absence of IOP reflects the fact that these genes must be expressed in cells devoid of *dio3*, such as in the ventral zone.

A final point is that the *p_{dio3}*-GFP reporter tadpoles are a useful tool for following *dio3* expressing cells and for displaying the regulation of TH availability by D3 at the cellular scale. Moreover, the expression level of *dio3* and the reporter gene are reasonably well correlated, despite a certain variability due to the very dynamic D3 expression at specific stages, a fact that could be compounded by the difficulty of obtaining homogeneous batches of tadpoles. However, even if *dio3* is transcriptionally responsive to T_3 , its range of T_3 -responsiveness is far below that of the *TH/bZIP*. As such the *TH/bZIP* reporter remains the best T_3 -sensor available to date in xenopus.

Conclusions

Our findings show that *dio3* displays a dynamic and cell-specific expression in the pre-metamorphic retina between NF41 and NF48. At stage NF41 and NF48 most cells types express *dio3*, with a particularly high expression in rods and the S cones at NF48 whereas T_3 signaling is detectable in horizontal neurons and ganglion cells (Fig 5). After metamorphosis, *dio3* expression was much more limited, only being found in amacrine cells and a sub-population of photoreceptors. The results show that *dio3* plays a key role in determining TH availability during retinal development with a precise and cell-type specific timing. We suggest that D3 expression could be necessary to protect photoreceptors and bipolar neurons from out of phase TH signaling and hence that *dio3* expression constrains effects of TH signaling in the retina prior to and during metamorphosis.

Acknowledgments

We thank the IJM imaging platform (ImagoSeine facility, member of the France BioImaging infrastructure supported by the French National Research Agency (ANR-10-INSB-04, « Investments of the future »). We thank Yorick Gitton for insightful and valuable comments. We thank Michelle Leemans for the primers design and Louise Péricard for technical advice for quantitative real time PCR. The excellent animal care provided by Gérard Benisti and Philippe Durand is gratefully acknowledged.

This work was supported by the Centre National de la Recherche Scientifique (CNRS), the Museum National d'Histoire Naturelle (MNHN), the French ANR "Thrust", Agence Nationale de la Recherche (11BSV2019 02) and a PERSU grant (SU-14-R-PERSU-04) to BAD. Laetitia Préau received a PhD grant from the French Ministry of Research and Education and support from the PERSU grant (Ministère de l'Éducation Nationale, de l'Enseignement Supérieur et de la Recherche) (SU-14-R-PERSU-04) to BAD. The funders had no role in study design, data collection and analysis, decision to publish, or preparation of the manuscript.

Author Contributions

Conceptualization: Karine Le Blay, Laëtitia Préau, Ghislaine Morvan-Dubois, Barbara Demeneix.

Data curation: Karine Le Blay, Ghislaine Morvan-Dubois, Barbara Demeneix.

Formal analysis: Karine Le Blay, Ghislaine Morvan-Dubois, Barbara Demeneix.

Funding acquisition: Ghislaine Morvan-Dubois, Barbara Demeneix.

Investigation: Karine Le Blay, Laëtitia Préau, Ghislaine Morvan-Dubois.

Methodology: Karine Le Blay, Laëtitia Préau, Ghislaine Morvan-Dubois, Barbara Demeneix.

Project administration: Barbara Demeneix.

Resources: Ghislaine Morvan-Dubois, Barbara Demeneix.

Supervision: Ghislaine Morvan-Dubois, Barbara Demeneix.

Validation: Karine Le Blay, Laëtitia Préau, Ghislaine Morvan-Dubois, Barbara Demeneix.

Visualization: Karine Le Blay.

Writing – original draft: Karine Le Blay, Laëtitia Préau, Ghislaine Morvan-Dubois, Barbara Demeneix.

Writing – review & editing: Karine Le Blay, Ghislaine Morvan-Dubois, Barbara Demeneix.

References

1. Bernal J, Guadaño-Ferraz A, Morte B. Perspectives in the study of thyroid hormone action on brain development and function. *Thyroid*. 2003; 13(11):1005–12. <https://doi.org/10.1089/105072503770867174> PMID: 14651784.
2. Harpavat S, Cepko CL. Thyroid hormone and retinal development: an emerging field. *Thyroid*. 2003; 13(11):1013–9. <https://doi.org/10.1089/105072503770867183> PMID: 14651785.
3. Ng L, Hurley JB, Dierks B, Srinivas M, Saltó C, Vennström B et al. A thyroid hormone receptor that is required for the development of green cone photoreceptors. *Nat Genet*. 2001; 27(1):94–8. <https://doi.org/10.1038/83829> PMID: 11138006.
4. Havis E, Le Mevel S, Morvan Dubois G, Shi DL, Scanlan TS, Demeneix BA et al. Unliganded thyroid hormone receptor is essential for *Xenopus laevis* eye development. *EMBO J*. 2006; 25(20):4943–51. Epub 2006/09/28. <https://doi.org/10.1038/sj.emboj.7601356> PMID: 17006540; PubMed Central PMCID: PMC1618110.
5. Houbrechts AM, Vergauwen L, Bagci E, Van Houcke J, Heijnen M, Kulemeka B et al. Deiodinase knock-down affects zebrafish eye development at the level of gene expression, morphology and function. *Mol Cell Endocrinol*. 2016; 424:81–93. Epub 2016/01/21. <https://doi.org/10.1016/j.mce.2016.01.018> PMID: 26802877.
6. Darras VM, Mol KA, van der Geyten, Kühn ER. Control of peripheral thyroid hormone levels by activating and inactivating deiodinases. *Ann N Y Acad Sci*. 1998; 839:80–6. PMID: 9629134.
7. Nunez J, Celi FS, Ng L, Forrest D. Multigenic control of thyroid hormone functions in the nervous system. *Mol Cell Endocrinol*. 2008; 287(1–2):1–12. Epub 2008/03/25. <https://doi.org/10.1016/j.mce.2008.03.006> PMID: 18448240; PubMed Central PMCID: PMC1618110.
8. Préau L, Le Blay K, Saint Paul E, Morvan-Dubois G, Demeneix BA. Differential thyroid hormone sensitivity of fast cycling progenitors in the neurogenic niches of tadpoles and juvenile frogs. *Mol Cell Endocrinol*. 2016; 420:138–51. Epub 2015/11/26. <https://doi.org/10.1016/j.mce.2015.11.026> PMID: 26628040.
9. Houbrechts AM, Delarue J, Gabriëls IJ, Sourbron J, Darras VM. Permanent Deiodinase Type 2 Deficiency Strongly Perturbs Zebrafish Development, Growth, and Fertility. *Endocrinology*. 2016; 157(9):3668–81. Epub 2016/07/20. <https://doi.org/10.1210/en.2016-1077> PMID: 27580812.
10. Kelley MW, Turner JK, Reh TA. Ligands of steroid/thyroid receptors induce cone photoreceptors in vertebrate retina. *Development*. 1995; 121(11):3777–85. PMID: 8582287.
11. Marsh-Armstrong N, Huang H, Remo BF, Liu TT, Brown DD. Asymmetric growth and development of the *Xenopus laevis* retina during metamorphosis is controlled by type III deiodinase. *Neuron*. 1999; 24(4):871–8. PMID: 10624950.
12. Ng L, Lyubarsky A, Nikonov SS, Ma M, Srinivas M, Kefas B et al. Type 3 deiodinase, a thyroid-hormone-inactivating enzyme, controls survival and maturation of cone photoreceptors. *J Neurosci*. 2010; 30(9):3347–57. <https://doi.org/10.1523/JNEUROSCI.5267-09.2010> PMID: 20203194; PubMed Central PMCID: PMC1618110.
13. Brown DD. The role of deiodinases in amphibian metamorphosis. *Thyroid*. 2005; 15(8):815–21. <https://doi.org/10.1089/thy.2005.15.815> PMID: 16131324.
14. Ma H, Ding XQ. Thyroid Hormone Signaling and Cone Photoreceptor Viability. *Adv Exp Med Biol*. 2016; 854:613–8. https://doi.org/10.1007/978-3-319-17121-0_81 PMID: 26427466.

15. Bilitou A. and Ohnuma S. The role of cell cycle in retina development: Cyclin- dependent kinase inhibitors co-ordinate cell cycle inhibition, cell-fate determination and differentiation in the developing retina. *Developmental Dynamics* 2010 Mar; 239:727–736. <https://doi.org/10.1002/dvdy.22223> PMID: 20108332
16. Álvarez-Hernán G, Bejarano-Escobar R, Morona R, González A, Martín-Partido G, Francisco-Morcillo J. Islet-1 immunoreactivity in the developing retina of *Xenopus laevis*. *Hindawi Publishing Corporation The ScientificWorld Journal* Volume 2013, Article ID 740420. <https://doi.org/10.1155/2013/740420>
17. Bessodes N, Parain K, Bronchain O, Bellefroid EJ, Perron M. Prdm13 forms a feedback loop with Ptf1a and is required for glycinergic amacrine cell genesis in the *Xenopus* Retina. *Neural Development* (2017) 12:16. <https://doi.org/10.1186/s13064-017-0093-2> PMID: 28863786
18. D'Autilia S, Decembrini S, Casarosa S, He RQ, Barsacchi G, Cremisi Fet al. Cloning and developmental expression of the *Xenopus* homeobox gene *Xvsx1*. *Dev Genes Evol* (2006) 216:829–834. <https://doi.org/10.1007/s00427-006-0109-0> PMID: 17103185
19. Dullin JP, Locker M, Robach M, Henningfeld KA, Parain K, Afelik Set al. Ptf1a triggers GABAergic neuronal cell fates in the retina. *BMC Developmental Biology BMC Developmental Biology* 2007, 7:110. <https://doi.org/10.1186/1471-213X-7-110> PMID: 17910758
20. Chang WS, Harris WA. Sequential genesis and determination of cone and rod photoreceptors in *Xenopus*. *J Neurobiol.* 1998 Jun; 35(3):227–44. PMID: 9622007
21. Parker RO, Mccarragher B, Crouch R, Darden AG. Photoreceptor development in premetamorphic and metamorphic *Xenopus laevis*. *Anat Rec (Hoboken)*. 2010 Mar; 293(3):383–7. <https://doi.org/10.1002/ar.21079> PMID: 20091886
22. Fini JB, Le Mével S, Palmier K, Darras VM, Punzon I, Richardson SJet al. Thyroid hormone signaling in the *Xenopus laevis* embryo is functional and susceptible to endocrine disruption. *Endocrinology*. 2012; 153(10):5068–81. Epub 2012/09/11. <https://doi.org/10.1210/en.2012-1463> PMID: 22968643.
23. Fini JB, Le Mevel S, Turque N, Palmier K, Zalko D, Cravedi JP et al. An in vivo multiwell-based fluorescent screen for monitoring vertebrate thyroid hormone disruption. *Environ Sci Technol.* 2007; 41(16):5908–14. PMID: 17874805.
24. Turque N, Palmier K, Le Mével S, Alliot C, Demeneix BA. A rapid, physiologic protocol for testing transcriptional effects of thyroid-disrupting agents in premetamorphic *Xenopus* tadpoles. *Environ Health Perspect.* 2005; 113(11):1588–93. <https://doi.org/10.1289/ehp.7992> PMID: 16263516; PubMed Central PMCID: PMC1310923.
25. Amaya E, Kroll KL. A method for generating transgenic frog embryos. *Methods Mol. Biol.* 1999; 97:393–414. <https://doi.org/10.1385/1-59259-270-8:393> PMID: 10443381.
26. Cabochette P, Vega-Lopez G, Bitard J, Parain K, Chemouny R, Masson C et al. YAP controls retinal stem cell DNA replication timing and genomic stability. *eLIFE.* 2015; 4:e08488. <https://doi.org/10.7554/eLife.08488> PMID: 26393999
27. Wong LL, Rapaport DH. Defining retinal progenitor cell competence in *Xenopus laevis* by clonal analysis. *Development.* 2009; 136(10):1707–15. <https://doi.org/10.1242/dev.027607> PMID: 19395642; PubMed Central PMCID: PMC2673759.
28. Pessôa CN, Santiago LA, Santiago DA, Machado DS, Rocha FA, Ventura DF et al. Thyroid hormone action is required for normal cone opsin expression during mouse retinal development. *Invest Ophthalmol Vis Sci.* 2008; 49(5):2039–45. <https://doi.org/10.1167/iovs.07-0908> PMID: 18436838.
29. Roberts MR, Srinivas M, Forrest D, Morreale de Escobar G, Reh TA. Making the gradient: thyroid hormone regulates cone opsin expression in the developing mouse retina. *Proc Natl Acad Sci U S A.* 2006; 103(16):6218–23. Epub 2006/04/10. <https://doi.org/10.1073/pnas.0509981103> PMID: 16606843; PubMed Central PMCID: PMC1458858.
30. Tata JR. Amphibian metamorphosis as a model for the developmental actions of thyroid hormone. *Mol Cell Endocrinol.* 2006; 246(1–2):10–20. Epub 2006/01/04. <https://doi.org/10.1016/j.mce.2005.11.024> PMID: 16413959.
31. Leloup J., Buscaglia M., 1977. La triiodothyronine, hormone de la metamorphose des amphibiens. *C. R. Acad. Sci.* 84, 2261–2263.
32. Cossette SM, Drysdale TA. Early expression of thyroid hormone receptor beta and retinoid X receptor gamma in the *Xenopus* embryo. *Differentiation.* 2004; 72(5):239–49. <https://doi.org/10.1111/j.1432-0436.2004.07205006.x> PMID: 15270780.
33. Mader MM, Cameron DA. Effects of induced systemic hypothyroidism upon the retina: regulation of thyroid hormone receptor alpha and photoreceptor production. *Mol Vis.* 2006; 12:915–30. Epub 2006/08/11. PMID: 16917485.
34. Raine JC, Hawryshyn CW. Changes in thyroid hormone reception precede SWS1 opsin downregulation in trout retina. *J Exp Biol.* 2009; 212(17):2781–8. <https://doi.org/10.1242/jeb.030866> PMID: 19684211.

35. Sjöberg M, Vennström B, Forrest D. Thyroid hormone receptors in chick retinal development: differential expression of mRNAs for alpha and N-terminal variant beta receptors. *Development*. 1992; 114(1):39–47. PMID: [1576965](https://pubmed.ncbi.nlm.nih.gov/1576965/).
36. Allison WT, Dann SG, Veldhoen KM, Hawryshyn CW. Degeneration and regeneration of ultraviolet cone photoreceptors during development in rainbow trout. *J Comp Neurol*. 2006; 499(5):702–15. <https://doi.org/10.1002/cne.21164> PMID: [17048226](https://pubmed.ncbi.nlm.nih.gov/17048226/).
37. Browman HI, Hawryshyn CW. Thyroxine induces a precocial loss of ultraviolet photosensitivity in rainbow trout (*Oncorhynchus mykiss*, Teleostei). *Vision Res*. 1992; 32(12):2303–12. PMID: [1288007](https://pubmed.ncbi.nlm.nih.gov/1288007/).
38. Browman HI, Hawryshyn CW. The developmental trajectory of ultraviolet photosensitivity in rainbow trout is altered by thyroxine. *Vision Res*. 1994; 34(11): 1397–406. PMID: [8023449](https://pubmed.ncbi.nlm.nih.gov/8023449/).
39. Raine JC, Coffin AB, Hawryshyn CW. Systemic thyroid hormone is necessary and sufficient to induce ultraviolet-sensitive cone loss in the juvenile rainbow trout retina. *J Exp Biol*. 2010; 213(3):493–501. <https://doi.org/10.1242/jeb.036301> PMID: [20086135](https://pubmed.ncbi.nlm.nih.gov/20086135/).